Materials Science & Engineering A 699 (2017) 48–54

Contents lists available at ScienceDirect

Materials Science & Engineering A

journal homepage: www.elsevier.com/locate/msea

Microstructure and local strains in GH3535 alloy heat affected zone and their influence on the mechanical properties

Shuangjian Chen[a,b], D.K.L. Tsang[a], Li Jiang[a,b], Kun Yu[a,b], Chaowen Li[a], Zhong Li[a], Zhijun Li[a,*], Xingtai Zhou[a], Jianguo Yang[c]

[a] Center for Thorium Molten Salt Reactor System, Shanghai Institute of Applied Physics, Chinese Academy of Sciences, Shanghai 201800, PR China
[b] University of Chinese Academy of Sciences, Beijing 100049, PR China
[c] Zhejiang University of Technology, Hangzhou 310014, PR China

ARTICLE INFO

Keywords:
EBSD
Twinning
Dislocations
Nickel based superalloys
Welding
Hardening

ABSTRACT

GH3535 alloy plates were welded by Gas Tungsten Arc Welding in order to study the evolution of microstructure and mechanical properties in the heat-affected zone (HAZ). Our results suggest that welding thermal cycles induced the morphology evolution of M_6C carbides from block to eutectic near the fusion line in the HAZ. Electron backscatter diffraction (EBSD) results show that significant amounts of plastic strains occurred in the HAZ after welding. In addition, local coherent twin boundaries (Σ3) and dislocations were observed to decrease with the distance from the fusion line. Mechanical tests indicate that the hardness, yield strength and ultimate strength in HAZ are higher than those in base metal, and their values decrease with the distance from the fusion line. However, the elongation increases as the strengths decrease. The higher strength and lower elongation in the HAZ are mainly attributed to residual strains with the function of strain-hardening. Moreover, the change of Σ3 boundary which is in good agreement with that of elongation suggests a positive influence on the plastic deformation.

1. Introduction

Ni-Mo-Cr alloys have been widely used in aerospace, chemical and nuclear industries due to their high corrosion resistance, superior strength at room and elevated temperatures [1–5]. To date, extensive studies have been carried out on Ni-Mo-Cr alloys. These studies are mainly focused on weld properties [6,7] in view of the fact that a welded joint is normally a weakest part in a welded component. The residual strains and changes of material properties such as local microstructure, chemical composition and carbide distribution may also occur in the heat-affected zone (HAZ) during the multiple welding thermal cycles [8,9]. Residual strain-hardening is considered to be a main factor to lead to heterogeneous mechanical performance and some potential problems [10–12]. Previous study on Alloy 690TT revealed that strain-hardening resulting from weld shrinkage increases the micro-hardness in the HAZ and sequentially promotes corrosion cracking sensitivity at high temperatures [11,13]. Ductility-dip crack can also easily occur in the HAZ for some Ni-Mo-Cr alloys with high concentration of carbon and alloy elements [14–16]. Uneven grain boundary is another important factor which can affect the mechanical properties in the HAZ in nickel base alloy, Σ3 boundaries is reported to be very helpful to prevent intergranular cracking and expansion of elongation [17,18].

As a representative Ni–Mo–Cr solid solution strengthened alloy developed by Oak Ridge National Laboratory (ORNL), Hastelloy N alloy (UNS N10003) has been used as a main structural material for Molten Salt Reactor in 1960s [19] and Thorium Molten Salt Reactor (TMSR) in 2010s [20,21], which serves at elevated temperatures between 650 °C and 750 °C [22–24]. To our best knowledge, no works on detailed investigation of local strains and grain boundaries in the HAZ and its influence on the mechanical performance have been reported to date. In this work, we have investigated the effect of welding thermal cycle on the microstructure and mechanical properties of HAZ. Samples were cut from the HAZ to study the evolution process of microstructure and mechanical properties. The hardness, tensile properties, microstructure properties in terms of distribution of precipitations, grain sizes, dislocations and grain boundaries character parameters such as fractions of Σ3 boundary, distribution of kernel average misorientation (KAM) in Alloy GH3535 (UNS N10003) HAZ were characterized. Furthermore, the relationship between the microstructure properties and mechanical properties in both HAZ and base metal were studied.

* Corresponding author.
E-mail address: lizhijun@sinap.ac.cn (Z. Li).

http://dx.doi.org/10.1016/j.msea.2017.05.072
Received 27 January 2017; Received in revised form 18 May 2017; Accepted 19 May 2017
Available online 20 May 2017

Table 1
Chemical compositions of GH3535 alloy and filler wire (wt%).

Alloy	Mo	Cr	Fe	C	Si	Mn	Ni
GH3535	16.5	7.0	4.0	0.06	0.27	0.5	Bal.
ERNiMo-2	16.4	8.0	5.0	0.05	1	1	Bal.

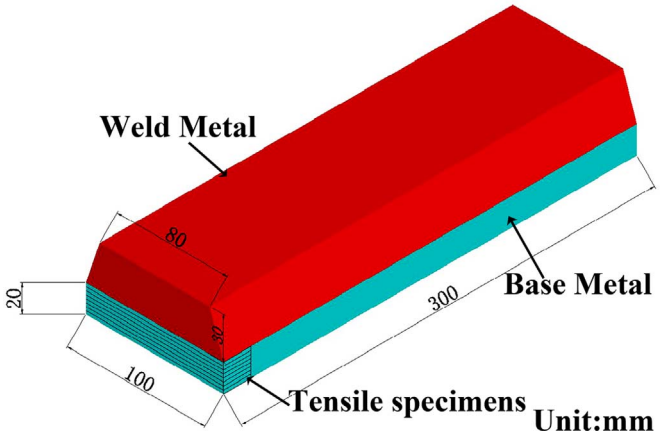

Fig. 1. Weldment schematic and locations of tensile specimens in parent alloy.

2. Experimental procedure

The weldment was prepared by Gas Tungsten Arc Welding by using two GH3535 alloy plates with each thickness of 20 mm and ERNiMo-2 filler wire with a diameter of 1.2 mm. The nominal chemical compositions of the parent alloy and the filler wire are listed in Table 1. 2% Cerium Tungsten electrode with a diameter of 2.4 mm and high purity Argon (99.99%) were applied as welding consumable. A cladding layer with a thickness of 30 mm was buttered on the surface of GH3535 alloy plate. The detailed welding parameters were: welding current 280 A, pulse frequency 2.5 Hz, peak pulse duration 50% and base value/peak value 50%, welding speed 90 mm/min. Fig. 1 shows the schematic of the weldment of GH3535 alloy.

Microstructure was characterized on a Zeiss LEO 1530VP scanning electron microscope (SEM) equipped with energy dispersive spectroscopy (EDS). The grain boundary character and the local strains distributions in the HAZ were analyzed by an Oxford electron backscattered diffraction (EBSD) system with the Aztec software. KAM is the average misorientation between every pixel and its surrounding pixels in the EBSD measurements, which can estimate the local strains and represent the density of geometrically necessary dislocation (GND) in crystalline materials [9,25]. Samples for EBSD were cut from the HAZ and processed by vibration polishing for 2 h with 0.5 μm diamond paste to remove surface stress. EBSD data post-processing was done with Aztec software packages. The whole EBSD experiment process is as follows. (1) Samples for EBSD were processed by vibration polishing for 2 h with 0.5 μm diamond paste to remove surface stress. The acceleration voltage and current were set as 20 kV and 100 mA respectively. EBSD mapping were carried out within an area of 300*500 μm^2 with a step size of 1 μm. (2) EBSD maps were processed by noise reduction after mapping. (3) Corresponding histograms and data of circle equivalent grain size distribution, KAM were calculated automatically from EBSD maps.

Vickers hardness in the HAZ was measured on a ZHV 30 micro Vickers with a load of 500 gf and a holding time of 15 s. Eight tensile specimens with a thickness of 2 mm were sampled from both HAZ and base metal along the thickness direction as shown in Fig. 1.

The geometry of tensile specimens is depicted in Fig. 2. The tensile tests with a set of 2 specimens were performed on a Zwick Z100 universal testing machine at two temperatures 25 °C and 700 °C. The strain rates were set as 0.005/min and 0.05/min before and after the yield point, according to ASTM E8 [26] and ASTM E21 [27], respectively.

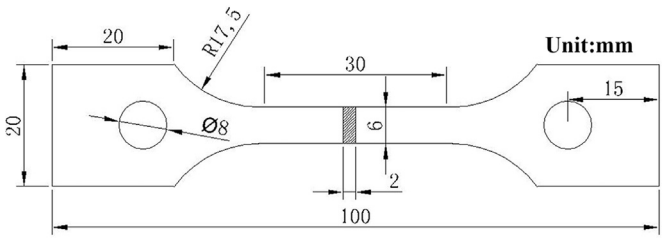

Fig. 2. Dimensions of the tensile specimens.

3. Results

3.1. Microstructure evolution and residual strains in the HAZ and base metal

Microstructure of the HAZ near the fusion line was observed by SEM as shown in Fig. 3. The region near the fusion line as shown in Fig. 3(a) can be divided into three parts, namely, weld, HAZ(E) and HAZ(R). HAZ(E) stands for the region where primary M_6C (Location A) carbides have transformed into eutectic carbides (Location B), and HAZ(R) stands for the rest of the HAZ without carbides transformation. In addition, Fig. 3(a) shows that the area with significant microstructure change is approximately in the range of 400 μm from the fusion line. Fig. 3(b) shows a greater magnification of HAZ(E) where two forms of eutectic carbides are observed. One is lamellar structure (Location B) as shown in Fig. 3(b) and (d). The other one close to the fusion line is spheroidized carbides (Location C) consisting of fine particles and small rod-like as shown in Fig. 3(e). The lamellar structure carbides (Location B) is the production of eutectic reaction of primary carbides which occurred when peak temperature of the thermal cycle over 1300 °C [28] during welding. The type of lamellar carbides seems to be stable when the heat input is small, however, in the cladding process, they can occur spheroidization and turn into carbides with the structure of fine particles and small rod-like under the influence of multiple repeated welding thermal cycles with high peak temperatures.

To further investigate the influence of welding process on the microstructure of HAZ, several regions with different distances from the fusion line (X = 0.5–20 mm) were characterized by SEM to investigate the microstructure evolution. As shown in Fig. 4(a)–(h), the eight local regions possess similar microstructure, the sizes of primary M_6C in the HAZ are all in the range from 3 μm to 10 μm. Precipitates in the grain boundaries are observed in the whole HAZ and base metal. In general, there are no significant changes on the microstructure in the region within 0.5–20 mm from the fusion line.

The grain boundary character maps, all-Euler maps, kernel average misorientation (KAM) distribution maps and the grain boundary character distribution of the HAZ analyzed by EBSD are shown in Figs. 5–7, respectively, as a function of distance from the fusion line. Eight samples were taken from the HAZ and base metal for the EBSD experiment, the distances of sample locations from the fusion line were 0 mm, 1 mm, 2 mm, 3 mm, 4 mm, 5 mm, 10 mm, 20 mm, respectively. Figs. 5(a) and 6(a) show that the grain size generally decreases with the distance from the fusion line. The average grain size near the fusion line (X = 0 mm) is 38 μm, approximately 5 μm larger than at location X = 20 mm. Figs. 5(b) and 6(b) show that Σ3 boundaries increase with the distance from the fusion line. And the frequency of Σ3 boundaries goes up from 19.2% (X = 0 mm) to about 40% (X = 20 mm).

The KAM map can be used to access the residual strains [29]. Blue and red colors in Fig. 5(c) represent the minimum and the maximum KAM values, respectively. The color of the KAM near the fusion line (X = 0 mm) is much brighter, indicating the residual strain in this region